Hindawi
Wireless Communications and Mobile Computing
Volume 2021, Article ID 5371330, 15 pages
https://doi.org/10.1155/2021/5371330

Research Article

Universal Method for Constructing Fault-Tolerant Optical Routers Using RRW

Meaad Fadhel, Lei Huang, and Huaxi Gu

State Key Laboratory of Integrated Service Network, Xidian University, Xi'an, China

Correspondence should be addressed to Huaxi Gu; hxgu@xidian.edu.cn

Received 7 May 2021; Accepted 26 July 2021; Published 18 August 2021

Academic Editor: Yong Zhang

High-speed data transmission enabled by photonic network-on-chip (PNoC) has been regarded as a significant technology to overcome the power and bandwidth constraints of electrical network-on-Chip (ENoC). This has given rise to an exciting new research area, which has piqued the public's attention. Current on-chip architectures cannot guarantee the reliability of PNoC, due to component failures or breakdowns occurring, mainly, in active components such as optical routers (ORs). When such faults manifest, the optical router will not function properly, and the whole network will ultimately collapse. Moreover, essential phenomena such as insertion loss, crosstalk noise, and optical signal-to-noise ratio (OSNR) must be considered to provide fault-tolerant PNoC architectures with low-power consumption. The main purpose of this manuscript is to improve the reliability of PNoCs without exposing the network to further blocking or contention by taking the effect of backup paths on signals sent over the default paths into consideration. Thus, we propose a universal method that can be applied to any optical router in order to increase the reliability by using a reliable ring waveguide (RRW) to provide backup paths for each transmitted signal within the same router, without the need to change the route of the signal within the network. Moreover, we proposed a simultaneous transmission probability analysis for optical routers to show the feasibility of this proposed method. This probability analyzes all the possible signals that can be transmitted at the same time within the default and the backup paths of the router. Our research work shows that the simultaneous transmission probability is improved by 10% to 46% compared to other fault-tolerant optical routers. Furthermore, the worst-case insertion loss of our scheme can be reduced by 46.34% compared to others. The worst-case crosstalk noise is also reduced by 24.55%, at least, for the default path and 15.7%, at least, for the backup path. Finally, in the network level, the OSNR is increased by an average of 68.5% for the default path and an average of 15.9% for the backup path, for different sizes of the network.

1. Introduction

The on-chip networking fabric, generally introduced as networks-on-chip (NoCs), has become a restricting factor in terms of efficiency and power dissipation as the movement toward many-core processors proceeds [1, 2]. This is mostly due to electrical interconnects' intrinsic technical shortcomings in scaling energy and latency at the same level as transistors. As a result, the photonic network-on-chip was proposed as a potential networking architecture for future multiprocessor systems [3–5]. Photonic network-on-chip improves the intercore connectivity performance even more than ENoCs by using the advantages of silicon photonics technology, such as the high bandwidth, low end-to-end (ETE) delay, less energy consumption, and less crosstalk [6–8].

Topologies and optical routers are the most significant component of the photonic network-on-chip architecture. Therefore, several network topologies have been documented in the literature [9, 10]. One of the main components of photonic interconnects is optical routers, which connect a local core to the neighbouring nodes and are critical components in the development of a variety of photonic interconnections. As a result, they define the communication's precision and effectiveness. Many optical routers have been also reported in [11–14]. However, none of these designs provide an alternative path to transmit data when faults occur.

Faults can occur in any circuit, and photonic circuitries are not an exception. Although photonic networks are resilient to radiation-induced transient faults [15], it is still vulnerable to thermal variation (TV), process variation (PV), and ageing [16–18]. Process variation is affected by deviations from the manufacturing standard, which can lead to system failure. Moreover, active materials, as well as items with a high thermal variation, usually age more quickly [19]. Faults may occur in the microring resonators (MRs), waveguides, routers, and other optical components. Photodetectors, for example, have a higher failure rate compared to passive components like waveguides [19]. Furthermore, since a single MR failure will cause the entire message to be misrouted or lost, PNoCs are particularly susceptible to single-point failures. These misrouted or lost messages, even those small ones used for cache coherence, may have a huge impact on the network performance. This puts the reliability of communications in photonic network-on-chips in jeopardy. Since the system in critical mission applications must operate correctly under all conditions, high reliability is needed. This led many researchers to investigate the reliability of optical routers intensively [20–23], since they are the major active components of the network. However, the designs reported in these papers neglect the effect of backup paths on signals sent over the default paths.

In this manuscript, we propose a universal heuristic scheme to construct N-port fault-tolerant optical routers for photonic networks-on-chip. This scheme can be implemented to any size of optical routers to ensure the reliability of the network. This implementation does not expose the original optical router to some contention or further blocking issues. In this method, we implement a reliable ring waveguide with a restricted number of MRs to any optical router in order to provide a backup path for any unreliable port-to-port communication. Furthermore, signals sent over the provided backup path have no effect on signals sent over the main path within the original router. The suggested scheme is then used to optimize some of the most well-known optical routers for different topologies, such as mesh and torus topologies. This helps to decrease the failure probability of the optical router. This manuscript also proposes a simultaneous transmission analysis method for optical routers, which will show the feasibility of our proposed solution. In addition, we have made the following additional contributions to our previous work [24]: (1) in this manuscript, the RRW-based scheme mentioned in our previous work [24] is further modified to be more practical for different types of optical routers. (2) The proposed scheme is implemented to more types of nonreliable optical routers, as well as provide a case study. (3) In our previous work [24], we did not consider the reliability analysis of the optical router. In this work, we provide a detailed mathematical analysis and compare the failure probability of different fault-tolerant optical routers. (4) This manuscript introduces a mathematical simultaneous transmission analysis for optical routers to demonstrate that the blocking occurs while using the backup path provided by the fault-tolerant optical router architecture. (5) Unlike the previous conference version [24], this work uses a special simulator called VPIphotonics Design Suite (VPI) to simulate the optical router and provide analytical results such as insertion loss. (6) The previous work [24] only considers the router level evaluation. However, we consider the router and network level evaluation in this manuscript. As a conclusion, our major contributions in this manuscript are summarized as follows:

(i) Proposing a universal scheme architecture to build fault-tolerant optical routers from the standard original ones by using a reliable ring waveguide and limited number of MRs to increase the path diversity and provide backup paths

(ii) Providing a traffic configuration in RRW-based optical routers, along with a case study

(iii) Analysing the reliability parameters of different well-known optical routers using our proposed scheme

(iv) Developing a simultaneous transmission probability to prove the feasibility of our fault-tolerant scheme

(v) Improving the OSNR of the network. Our proposed RRW-based optical routers can improve network-level OSNR by an average of 68.5% for the default path and an average of 15.9% for the backup path under different network sizes

The rest of this manuscript has been organized as follows. We summarized the existing solutions for reliability issues in Section 2. The main structure of the proposed architecture and the traffic configuration are provided in Section 3. Section 4 presents a case study and illustrates the communication mechanism within routers using this scheme. Section 5 evaluates the proposed method compared to some other reliable optical routers for different network architectures; moreover, it analyzes the insertion loss and crosstalk noise of several routers in the router and network level.

2. Related Work

If one or more of an optical router's components fail for any reason, the optical router loses its effectiveness. The PNoC reliability issues have been discussed in a few papers. Since the system's reliability is endangered by a variety of factors, thus each of these papers has focused their efforts on one or more of these issues.

Thermal variance has a significant impact on the resonant wavelength of an MR, putting the reliability of on-chip interconnection in jeopardy. Via temperature profiling, Li et al. [25] investigated the effects of thermal change on the efficiency of on-chip optical data transmission. They also showed the relationship between temperature fluctuations, power usage, and contact reliability in PNoC. The authors in [26] suggested the SAFT-PHENIC, a thermal-aware fault-resilient hybrid optoelectrical on-chip interconnection. This paper reports a mesh-based fault-aware routing algorithm that is aimed at reducing thermal variance around the chip by using a traffic-aware approach to spread the load and avoid using some individual nodes. To mitigate defects, the authors of [22] suggested a low-power thermal-resilient

ONoC (RONoC) and studied the thermal variation of on-chip power delivery.

Process variation is the second major problem, which can lead to photonic system failure or inaccurate data transmission. The process variation is affected by critical physical fabrication defects caused by lithography imperfections and etch nonuniformity in photonic components [27]. Via proper arrangement among MRs and wavelengths with a low power requirement, an Integer Linear Programming (ILP) problem called "MinTrim" attempted to address the dilemma of wavelength shifting of MRs due to PV [28].

In PNoC, several academic papers deal with system-level fault-tolerant techniques. Rerouting the optical signal has been studied by several scholars [20, 21]. One disadvantage of this solution is that it often reroutes traffic in the same way that it induces traffic in one place, while ignoring the problematic routers entirely. The authors in [17, 29] suggested a fault-tolerant 3D ONoC with a smaller number of redundant MRs in very important paths. Furthermore, in [5, 23], the authors created a highly stable OR system for PNoCs. They expanded the number of alternative restore routes by adding minimal hardware redundancy to their previous OR, ensuring that standard communications could still be maintained. They also reported that their FTRA-NR fault-tolerant node reuse algorithm would find the best restore route within each faulty OR. Although both of the designs in [23, 29] increase the number of MRs for reliability purposes, they cause extra contention and insertion loss, since they use more resources (e.g., MRs) to reroute faulty signals in many cases. Similarly, the authors in [30] proposed a framework to construct fault-tolerant optical routers by using redundant MRs to provide extra paths. However, this framework is applied manually and does not have a regular rule to fit all types of optical routers, as well as provide more blocking as the previous two proposed ORs.

In this manuscript, we present a universal method for improving the reliability of any optical router without exposing it to any contention or blocking issues. This approach connects any optical router to a reliable ring waveguide with a small number of MRs as a backup path for any faulty port-to-port transmission. Furthermore, signals sent over the backup path have no effect on signals sent over the default path.

3. Fault-Tolerant Optical Router Architecture

3.1. Photonic Switching Elements. Optical routers have some irreplaceable elements such as MRs, waveguides, optical terminators (OTs), and basic switching elements (BSEs). OTs are optical devices that avoid the reflection of light in the waveguide. Waveguides act as a medium allowing optical signals to be transmitted from one port to another. They are the equivalent of wires in ENoCs. MRs are used to modulate optical signals as well as switch them. The combination of two waveguides and one or two MRs can construct a basic switching element. Depending on the location of the MRs and waveguides, the BSE can be a crossing switching element (CSE) or a parallel switching element (PSE) as shown in Figure 1. If an MR is connecting two parallel waveguides, it is called a PSE. Contrarily, if an MR or two MRs are connecting two crossed waveguides, it is called a CSE. If the MR connecting these two waveguides is powered on, it will have an on-state resonance wavelength λ_{on} and will switch any optical signal passing through it such as in Figures 1(b) and 1(d). Otherwise, if it is powered off, it will have an OFF-state resonance wavelength λ_{off} and the optical signal will pass through the MR without being switched as shown in Figures 1(a) and 1(c).

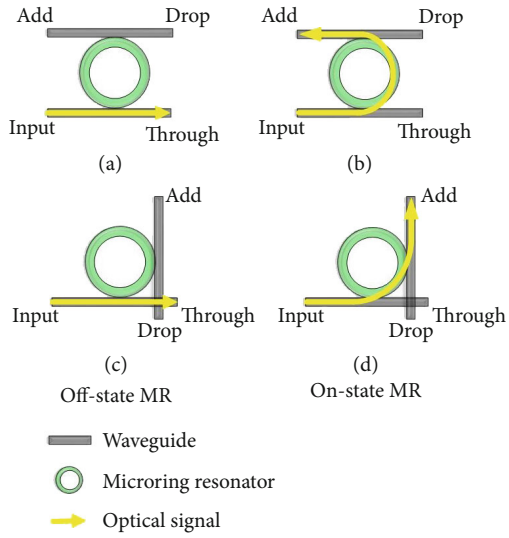

Figure 1: Basic switching elements: (a) off-state PSE, (b) on-state PSE, (c) off-state CSE, and (d) on-state CSE.

3.2. RRW Structure. The reliable ring waveguide is a universal scheme to construct fault-tolerant optical routers that guarantees a backup path for each faulty port-to-port communication within the same router. RRW scheme is constructed by implementing a single ring waveguide and some MRs to any optical router. If either of the original router's components malfunction for any reason, the ring waveguide serves as a backup path. The ring waveguide should be placed at the beginning and end of each input and output port, respectively, as seen in Figure 2(a). This avoids any possible contradictions with the original structure of the optical router while also simplifying the process. In addition, as seen in the figure, the MRs are located at each waveguide crossing created by the intersections of the ring waveguide and the input or output waveguides of the original optical router. Depending on the location of the input port and the output port regarding the port itself, the location of the MR is decided to be on the left side or the right side of the input/output waveguide of the port. Figures 2(a) and 2(b) show an example of both methods. When the input waveguide is located on the left side of the port and the output waveguide is on the right side of the port, one MR must be placed on the left side of the input waveguide of the port to provide an add point to the ring waveguide and another MR must be placed on the right side of the output waveguide of the port to create a drop point to the ring waveguide. Quite the opposite, if the input waveguide is located on the right side of the port and the output

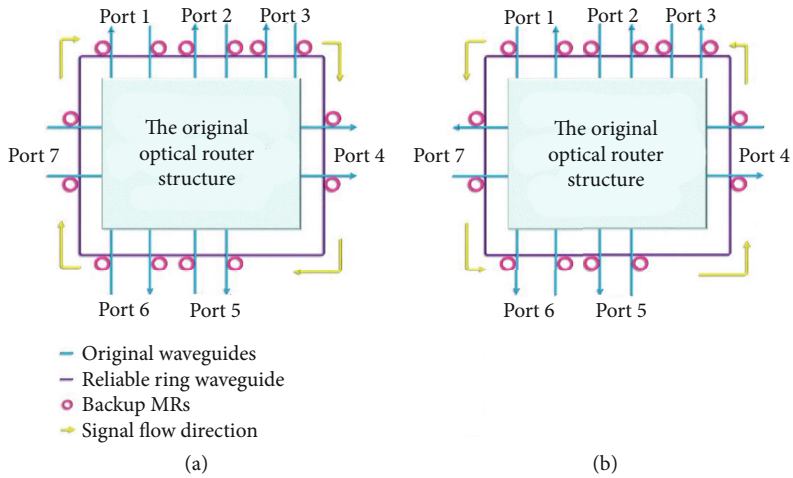

Figure 2: The reliable ring waveguide architecture: (a) clockwise RRW and (b) counterclockwise RRW.

waveguide is on the left side of the port, one MR must be located on the right side of the input waveguide of the port to work as an add point to the ring waveguide and another MR must be placed on the left side of the output waveguide of the port to act as a drop point to the ring waveguide. Drop points are where the MR downloads the signal inserted into another waveguide from the input waveguide, while add points are where the MR uploads the signal from another waveguide to the output waveguide [31].

It is worth mentioning that the location of the input and output waveguides regarding the port must be the same among the whole router in order to implement RRW properly. Moreover, depending on the location of the MR in regard to the input and output waveguides of each port, the data flow within the RRW is either clockwise or counterclockwise, but never both at the same time. When the MR is placed on the left side of the input waveguide and the right side of the output waveguide, the data flow will be clockwise. Otherwise, it will be counterclockwise as depicted in Figure 2(b).

Depending on the ports of the optical router, the total number of MRs in an $n \times n$ RRW-based optical router including the additional MRs is given by

$$\mathrm{MR}_{\mathrm{total}} = \mathrm{MR}_{\mathrm{org}} + 2n, \tag{1}$$

where $\mathrm{MR}_{\mathrm{org}}$ is the total number of MRs in the original optical router and n is the number of ports in the optical router. Furthermore, $2n$ is the number of MRs increased due to RRW scheme. Similarly, the total number of waveguides, waveguide crossings, waveguide bends, and optical terminators including the waveguides, waveguide crossings, and waveguide bends added by the ring waveguide is given by the following four equations, respectively:

$$W_{\mathrm{total}} = W_{\mathrm{org}} + 1, \tag{2}$$

$$C_{\mathrm{total}} = C_{\mathrm{org}} + 2n, \tag{3}$$

$$B_{\mathrm{total}} = B_{\mathrm{org}} + 4, \tag{4}$$

$$T_{\mathrm{total}} = T_{\mathrm{org}}, \tag{5}$$

where W_{org}, C_{org}, B_{org}, and T_{org} are the total number of waveguides, waveguide crossings, waveguide bends, and optical terminators utilized in the original optical router, respectively. Additionally, n is the number of ports in it, and $2n$ is the number of waveguide crossings increased after implementing the RRW scheme.

In case of component failure, the router will utilize the reliable ring waveguide to provide a backup path for data transmission, rather than using the default path. Furthermore, only a single signal is permitted to be transmitted alone the ring waveguide at a time. In other words, the reliable ring waveguide is only capable of transmitting one defective signal at a time. Lastly, the backup path's communications would never impact any other communications on the default path.

Given that the original optical router is strictly nonblocking, the only blocking that may happen would be either in the ring waveguide or at its intersections with the original router. However, our architecture ensures that it is implemented only at the beginning and end of each port, with an add point at the beginning of the input waveguide of a port and a drop point at the end of the output waveguide of the same port. As a result, it ensures that the add points are still ahead of the drop points to avoid overlapping [31].

This architecture offers an alternate path for the majority of faulty communication paths. In the router, each communication pair has two paths for data sharing. As a result, there is more route diversity for reliability purposes.

3.3. Traffic Configuration in RRW. In this subsection, we demonstrate how traffic is configured within RRW architecture. As previously mentioned, our architecture allows each router to function normally. Thus, we, here, illustrate that the signals flow within the RRW. Signals can be either propagated clockwise or counterclockwise, depending on the location of the MRs with regard to the input or output port. We here consider the case in which MRs are located at the left

side of the input waveguide and the right side of the output waveguide; thus, the flow of signals should be clockwise as shown in Figure 2(a).

For each port-to-port communication within RRW, the MR configuration is given as follows:

$$I_i \longrightarrow O_j : R_{2i}, R_{2j-1}, \tag{6}$$

where I_i is the input of i^{th} port and O_j is the output of j^{th} port. Furthermore, R_{2i} is the MR located at the input of the i^{th} port, and R_{2j-1} is the MR located at the output of the j^{th} port.

Since for any $n \times n$ optical router, the output matrix is given by Equation (7) or Equation (8):

$$\textbf{OUTPUT} = \textbf{switch matrix} \cdot \textbf{INPUT}, \tag{7}$$

$$\begin{bmatrix} O_1 \\ O_2 \\ O_3 \\ \vdots \\ O_n \end{bmatrix} = \textbf{switching matrix} \cdot \begin{bmatrix} I_1 \\ I_2 \\ I_3 \\ \vdots \\ I_n \end{bmatrix}. \tag{8}$$

According to Equation (8), the switching matrix of the backup bath in any $n \times n$ RRW-based optical router is presented as

$$\textbf{Switching matrix (RRW)} = \begin{bmatrix} 0 & R_2R_3 & R_2R_5 & \cdots & R_2R_{2n-1} \\ R_4R_1 & 0 & R_4R_5 & \cdots & R_4R_{2n-1} \\ R_6R_1 & R_6R_3 & 0 & \cdots & R_6R_{2n-1} \\ \vdots & \vdots & \vdots & \ddots & \vdots \\ R_{2n}R_1 & R_{2n}R_3 & R_{2n}R_5 & \cdots & 0 \end{bmatrix}. \tag{9}$$

Therefore, the matrix function of RRW is given by

$$\begin{bmatrix} O_1 \\ O_2 \\ O_3 \\ \vdots \\ O_n \end{bmatrix} = \begin{bmatrix} 0 & R_2R_3 & R_2R_5 & \cdots & R_2R_{2n-1} \\ R_4R_1 & 0 & R_4R_5 & \cdots & R_4R_{2n-1} \\ R_6R_1 & R_6R_3 & 0 & \cdots & R_6R_{2n-1} \\ \vdots & \vdots & \vdots & \ddots & \vdots \\ R_{2n}R_1 & R_{2n}R_3 & R_{2n}R_5 & \cdots & 0 \end{bmatrix} \cdot \begin{bmatrix} I_1 \\ I_2 \\ I_3 \\ \vdots \\ I_n \end{bmatrix}, \tag{10}$$

where 0 denotes that there is no communication between these ports, since no U-turns are allowed. U-turns are the turns in which the signal is transmitted from the input of a port to the output of the same port. Moreover, R is the ON-state MRs along RRW to establish a backup path from any one particular port to any other particular port. In the absence of faults, the signal will be transmitted according to the original switching matrix of the router itself. The following section will further illustrate this switching mechanism and MR configuration of RRW.

4. Case Study

In this section, we implement RRW in a well-known nonreliable optical router. Figure 3(a) presents an example of a nonreliable 5×5 optical router, proposed in [31], whereas Figure 3(b) shows the same OR after implementing our proposed scheme. As shown, the ring waveguide does not affect the functionality or connections of the original optical router yet increases the path diversity. Meanwhile, it adds some insertion loss and crosstalk to the original router, which is a slight increment compared to other reliable optical routers, as will be further illustrated in the following sections.

Since the input waveguide is located on the left side of the port and the output waveguide is on the right side of the port, we here use the method in Figure 2(a) to implement RRW into this router. MRs should be located on the left side of the input port and on the right side of the output port. Thus, the flow of signals is going on clockwise.

Given that this router has 15 original MRs, 15 waveguide crossings, and 5 waveguides, thus, according to Equation (1), the total number of MRs in this router after implementing RRW will be $\text{MR}_{\text{total}} = 15 + 2 \times 5 = 25$. Similarly, using Equation (2) and Equation (3), the total number of waveguides used is $W_{\text{total}} = 5 + 1 = 6$ and the total number of waveguide crossings will be $C_{\text{total}} = 15 + 2 \times 5 = 25$, respectively.

According to the labelled MRs in Figure 3(b), the switching matrix function of RRW in this 5×5 optical router is given as

$$\begin{bmatrix} O_1 \\ O_2 \\ O_3 \\ O_4 \\ O_5 \end{bmatrix} = \begin{bmatrix} 0 & R_2R_3 & R_2R_5 & R_2R_7 & w \\ w & 0 & R_4R_5 & R_4R_7 & R_4R_9 \\ R_6R_1 & w & 0 & R_6R_7 & R_6R_9 \\ R_8R_1 & R_8R_3 & w & 0 & R_8R_9 \\ R_{10}R_1 & R_{10}R_3 & R_{10}R_5 & w & 0 \end{bmatrix} \cdot \begin{bmatrix} I_1 \\ I_2 \\ I_3 \\ I_4 \\ I_5 \end{bmatrix}, \tag{11}$$

where 0 means no U-turn connections can be established and w means that waveguides are provided to realize this communication and thus no need for reliable MRs to realize it.

Furthermore, Table 1 lists all the possible communication pairs and denotes the corresponding MRs to realize them. The table presents the default paths as well as the reliable paths using RRW. The default path (also known as the original path) is presented first, then the reliable path (also known as the backup path). In the table, "w" signifies a path that does not require the activation of any MR, whereas "-" means a port cannot send itself. The table shows that for each communication pairs, there must be two paths at least. One of them is used as a backup path if and only if a malfunctioned MR is detected. For example, if port 2 is requesting to communicate with port 5 as shown in Figure 4, R_{16} should be turned on in order to switch the light signal from the input waveguide of port 2 to the output waveguide of port 5. However, in the presence of faulty MRs, the optical router has to take the backup path, which is represented by the reliable

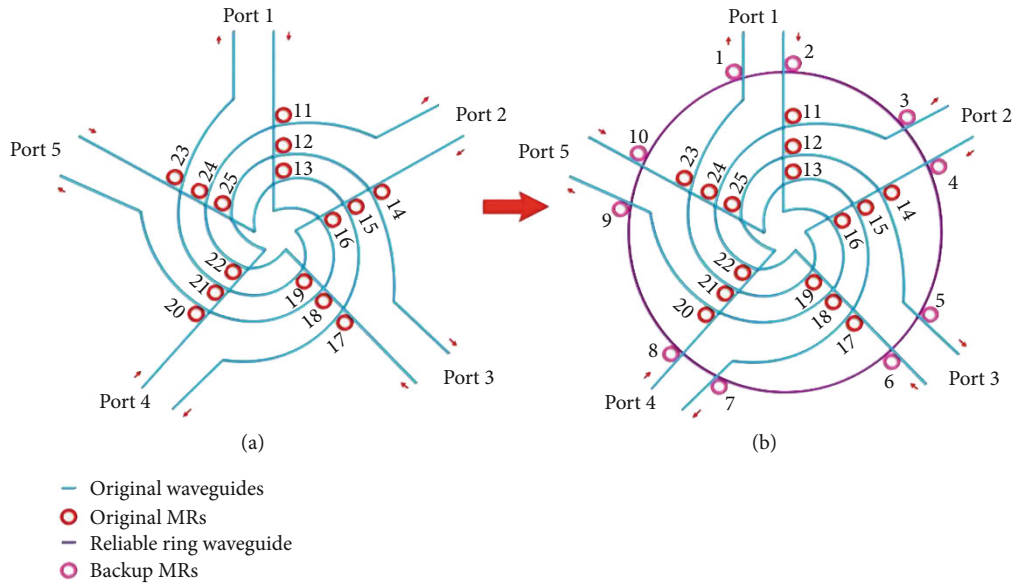

Figure 3: An example of implementing the reliable ring waveguide to the 5×5 optical router in [31].

Table 1: Resonator configuration in the 5×5 optical router proposed in [31] after implementing RRW.

From-to	Out 1	Out 2	Out 3	Out 4	Out 5
In 1	-	R_{11}; R_2, and R_3	R_{12}; R_2, and R_5	R_{13}; R_2, and R_7	w
In 2	w	-	R_{14}; R_4, and R_5	R_{15}; R_4, and R_7	R_{16}; R_4, and R_9
In 3	R_{19}; R_6, and R_1	w	-	R_{17}; R_6, and R_7	R_{18}; R_6, and R_9
In 4	R_{21}; R_8, and R_1	R_{22}; R_4, and R_3	w	-	R_{20}; R_8, and R_9
In 5	R_{23}; R_{10}, and R_1	R_{24}; R_{10}, and R_3	R_{25}; R_{10}, and R_5	w	-

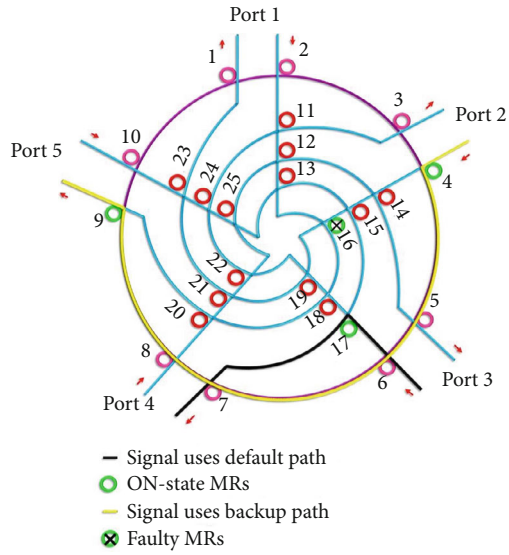

Figure 4: An example of communications in both the default and the backup paths in an RRW-based OR.

ring waveguide. Thus, two MRs should be switched on in order to transmit the light signal within the reliable ring waveguide. The exact MRs can be decided by Equation (6). Since in this case $i = 2$ and $j = 5$, the on-status MRs are R_4 and R_9. The light signal will be switched immediately using the first backup MR (i.e., R_4) and will be propagating along the reliable ring waveguide without interfering with the signals in the default paths, such as the signal transmitted from port 3 to port 4, until it will be coupled by R_9 to be ejected at the output of port 4. Therefore, RRW-based ORs are deemed to be nonblocking optical routers. Although in this case the backup path uses more resources and tend to have more insertion loss and crosstalk, this method can provide simultaneous transmission in the default path along with the backup path. In other words, this method does not disturb the normal flow of signals for reliability purposes. This will be further illustrated in the following section.

5. Performance Evaluation and Analysis

In this section, we evaluate the performance of RRW-based optical routers using the theoretical analysis and simulation evaluations using VPIphotonics Design Suite (VPI) [32].

To evaluate the performance of our architecture, we implement the reliable ring waveguide into several nonreliable optical routers proposed in [31, 33–38]; two of them are presented in Figure 5, and we compare them with 7×7 and 5×5 FTTDOR proposed in [29] and the NRFT optical router in [23] and some other fault-tolerant optical routers presented in [30].

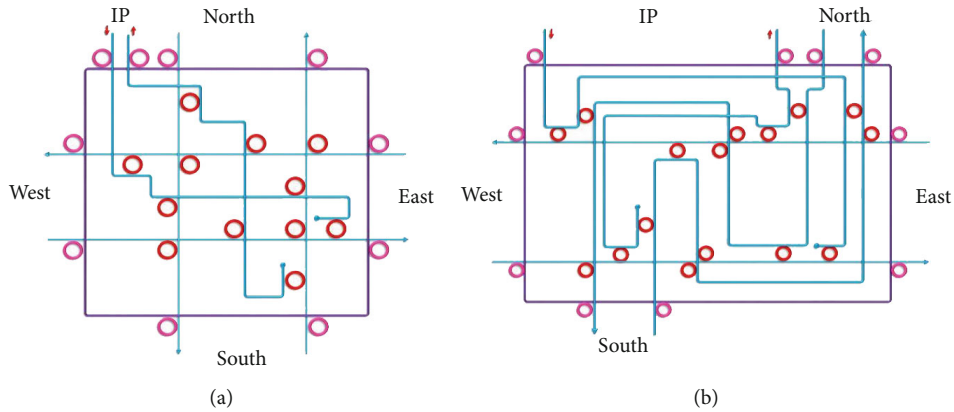

Figure 5: Some fault-tolerant optical routers based on RRW: (a) RRW-Crux and (b) RRW-Cygnus.

Table 2 compares the features of the proposed fault-tolerant scheme compared with some previously proposed fault-tolerant optical routers for different sizes. The table shows that RRW-based optical routers increase the reliability in the cost of increasing the number of MRs in some cases, especially when compared to 7×7 optical routers. However, RRW-based optical routers provide the least maximum number of ON-state MRs where a signal will pass through while traveling within the router in both the default and backup paths compared to other 7×7 optical routers. On the other hand, when compared to 5×5 optical routers, RRW-based optical routers have either the same number of additional backup MRs, such as in RRW-Crux and RRW-Cygnus, or less additional backup MRs, such as in RRW-crossbar. Similar to 7×7 optical routers, 5×5 RRW-based optical routers still provide the least maximum number of ON-state MRs where a signal passes through while being transmitted from one port to the other within the router.

5.1. Network Reliability Analysis. In this section, we analyze the reliability of the network using our design. The analysis is a modified version of the analysis presented in [23]. Moreover, this section shows the probability of our design functioning well, when the optical router is suffering from some faulty MRs. This can be evaluated using the following equation:

$$R_{\text{total}} = \prod_{i=1}^{N_w} \mathrm{R_w}(i) \times \prod_{j=1}^{N_{OR}} R_{\text{OR}}(j). \tag{12}$$

In this analysis, multiple faults are introduced into some MRs of the optical router in a random pattern, to examine whether the optical signals are properly received by the desired output port of the router or not. R_{total} is the entire network reliability; N_w and N_{OR} are the number of optical waveguides and the number of the optical routers used within the network, respectively. Similarly, R_w and R_{OR} denote the reliability of the i^{th} optical waveguide and the j^{th} optical router in the network, respectively. Unlike active components such as MRs, passive components such as waveguides are constantly in normal status and not prone to failures. Thus, the reliability of waveguides is the same throughout the network and can be ignored and set to be 1. Therefore, we neglect the optical waveguide reliability and focus on the reliability of optical routers within the network.

One major reason for optical router failures is a broken MR. Thus, given the reliability p of an MR (events of faulty MRs are independent of each other), the reliability of the optical router is given by

$$R_{\text{OR}} = 1 - \sum_{m=0}^{R} \partial_m \binom{R}{m} (1-p)^m (p)^{R-m}. \tag{13}$$

The number of simultaneously faulty MRs is denoted by m, whereas R represents the total number of MRs within the optical router (i.e., the MRs in the original router design and the backup MR added by RRW). Furthermore, the probability of an OR failure caused by m faulty MRs is presented by ∂_m.

Since our scheme uses the same optical router to tolerate physical faults occurring in the router, such as faults caused by thermal variations, the failure probability of our RRW-based optical router in the presence of m faulty MRs is illustrated as follows:

$$\partial_m = \frac{\sum_{k=1}^{P} \binom{MR_k}{m}}{\binom{R}{m}} \times 100\,(\%). \tag{14}$$

Equation (14) shows that the failure probability of an optical router is given by dividing the number of cases in which an optical signal is misrouted from its proper direction when one or several faulty MRs are introduced, by the cumulative number of cases in which m MRs out of an optical router's entire MRs (i.e., R, which includes both the original and the backup MRs) are unreliable. In the equation, k refers to the k^{th} path among the P sets of possible paths within the optical router, and MR_k denotes the number of MRs along the path k.

In most cases, when $m = 0$ or $m = 1$, i.e., no faulty MRs or only 1 faulty MR, the optical router still can manage to function as normal. This means that $\partial_0 = 0$ and $\partial_1 = 0$, since no misrouting is happening in the OR. However, when the number of faulty MRs increases to 2, i.e., $m = 2$, most fault-tolerant routers will start facing some misrouting difficulties, and when there are more than two faulty MRs, this

Table 2: Design features of several fault-tolerant optical routers compared to RRW-based scheme.

Routers	Default MRs	Additional MRs	Total MRs	Max. No. ON-MRs (default)	Max. No. ON-MRs (backup)
7×7 RO-Uni	26	14	40	1	2
7×7 RO-Votex	24	14	38	1	2
7×7 FTTDOR	22	10	32	2	3
7×7 NRFT	20	8	28	4	5
5×5 RRW-crossbar	20	10	30	1	2
5×5 FT-crossbar	20	13	33	1	3
5×5 RRW-ODOR	12	10	22	1	2
5×5 FT-ODOR	12	10	22	1	3
5×5 RRW-Crux	12	10	22	1	2
5×5 FT-Crux	12	10	22	1	3
5×5 RRW-Cygnus	16	10	26	1	2
5×5 FT-Cygnus	16	10	26	1	3

phenomenon is referred to as a state–space explosion problem. Thus, we here present the failure probability of different optical routers when 2 faulty MRs occur in the router.

Depending on the position of the faulty MR, the failure probability can be increased or decreased drastically. As a result, we computed all the possible positions for the faulty MRs (according to Table 1) and presented the average results in Figure 6. For instance, for RRW-based Cygnus, there exist 26 MRs, including 16 original MRs and 10 redundant MRs. The number of scenarios in which there exist two malfunctioned MRs is given by $\binom{26}{2}$. Moreover, there exist sixteen cases in which the signal is deflected due to the presence of two malfunctioned MRs. Therefore, the probability of failure of this router is $16/\binom{26}{2} = 4.9\%$. Accordingly, Figure 6 shows that RRW-based optical routers enjoy less failure probability compared to the 5×5 FTTDOR, which has the worst failure probability of 5.79%. On the other hand, the failure probability of RRW-Cygnus, RRW-Crossbar, RRW-Crux, RRW-ODOR, RRW-OXY, and RRW-OR is 4.9%, 4.59%, 5.19%, 5.19%, 5.19%, and 5.19%, respectively.

5.2. Simultaneous Transmission Analysis. Most of the proposed fault-tolerant optical router designs have addressed the reliability issue of the OR at the blocking expense. In other words, these architectures provide backup paths for most or all possible communication pairs; however, these backup paths block other default communication pairs within the optical router, which means that in several architectures, simultaneous transmission is not supported. Thus, in this manuscript, we propose a simultaneous transmission probability analysis for optical routers.

The probability of simultaneous transmission within the router using the default path can be calculated by obtaining the blocking probability of each possible communication pairs as follows:

$$T_{\text{sim}} = 1 - \frac{\sum_{i=1}^{P} (B/n)}{P}, \tag{15}$$

where T_{sim} is the simultaneous transmission in the router; i denotes the i^{th} path among P, which is the set of possible paths within the optical router; and (B/n) refers to the average probability of blocked paths out of all the possible simultaneous paths in the router, which is set to be n at most, for every $n \times n$ optical router. Since most of these optical routers are nonblocking architectures in general, we will only consider, here, the case of one faulty MR in the router, to check the possible simultaneous signal transmission within the router. For example, for FT-Crux, there is an average of 1.8 possible blocked default paths and there are 16 sets of possible paths in the router; thus, $T_{\text{sim}} = 1 - (1.8/16) = 0.887$.

Figure 7 depicts the probability of simultaneous signal transmission using the default path of several fault-tolerant routers and compares them to our scheme. It is so clear that NRFT suffers the most among other optical routers; this can be explained by the fact that this router is not a nonblocking router in general. This means that signals transmitted simultaneously within the router using default paths are blocking each other. On the other hand, most of the rest of the routers are nonblocking routers originally. However, since they use the same waveguides to transmit signals, blocking occurs, unlike RRW-based optical routers, because RRW-based optical routers are using the ring waveguide instead of the original waveguides in the router, which avoids conflicts and guarantees that the simultaneous signal transmission within the default path stays in a nonblocking state at all times.

5.3. Simulation Analysis. The simulation in this section is curried out using VPIphotonics Design Suite (VPI) [31]. The simulation results can illustrate the effect of various optical router design parameters, such as waveguide size and MR radius. As a result, this platform can provide simulation results that are closer to fabrication [39].

Table 3 demonstrates the parameter setting interface of all the four modules used to build the optical router considered in the case study and shown in Figure 3. These four modules are straight waveguide, waveguide bends, waveguide crossings, and crossing switching elements (CSEs).

Our simulation analysis is divided into three parts. First, we have simulated the original router without implementing

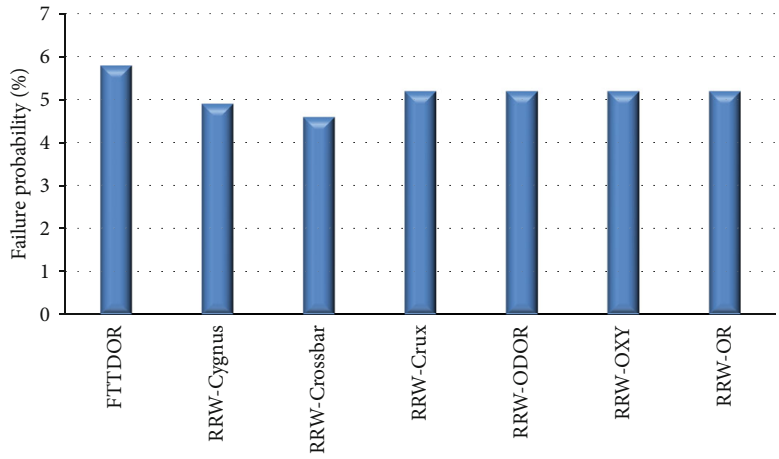

Figure 6: Failure probability of several fault-tolerant optical routers.

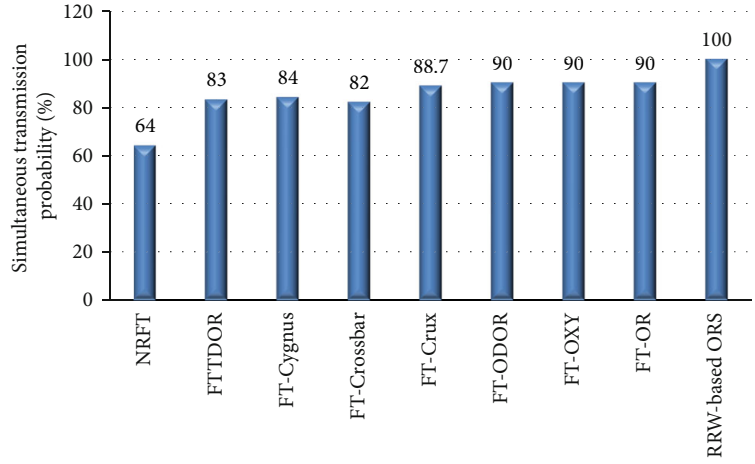

Figure 7: The probability of simultaneous signal transmission using the default path.

Table 3: The component parameters in the simulation environment.

Parameter	Value
Waveguide height	220 nm
Waveguide width	450 nm
Waveguide length	1 cm
Waveguide's refractive index	3.5
Surface roughness	10^{-9}
Radius of waveguide bends	5 μm
Radius of MRs	5 μm
Gap in CSEs	170 nm
Laser power	1 mW

the reliable ring waveguide scheme. As mentioned earlier and shown in Figure 3(a), the original optical router is made up of 15 MRs, 15 waveguide crossings, and 9 waveguide bends. According to the sequence of these components, we constructed the optical router using the corresponding module. In the simulation, we evaluate the insertion loss of each port-to-port communication. Figure 8 displays the worst-case insertion loss results, including power spectra for all of the five output ports. The worst-case IL occurs when the optical signal is traveling from the West port to the East port, since it passes through four OFF-state MRs, four waveguide crossings, one bend, and one ON-state MR. From the results shown in (Figure 8), the maximum insertion loss of the original optical router is -2.1 dB for optical signal at the frequency of 193.44 THz.

Second, we simulated the default path of the original router after implementing the reliable ring waveguide scheme. As depicted earlier in Figure 3(b), the RRW-based optical router has a total of 25 MRs, 25 waveguide crossings, and 13 waveguide bends. The RRW-based optical router is built up as shown in Figure 3. Figure 9 depicts the results of the worst-case insertion loss after evaluating all five communication pairs. The worst-case IL in RRW occurs when the optical signal is traveling from the West port to the East port as well, since it still passes through similar optical devices as the previously mentioned ones. The only difference is the 2 CSEs located at the beginning and the end of the default path. The results show that the maximum insertion loss of the RRW-based optical router when the optical signal is using the default path is -2.6 dB for optical signal at the frequency of 193.44 THz.

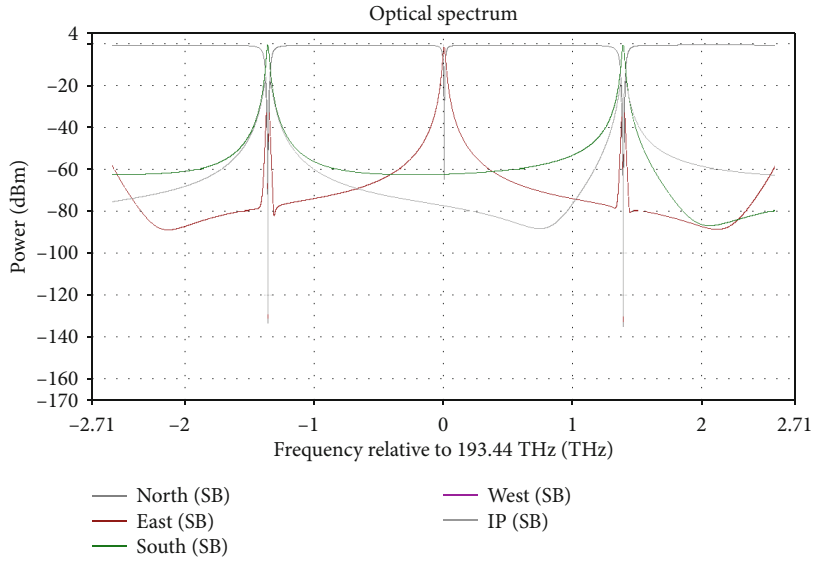

Figure 8: Power spectra of the optical router at all five output ports under the worst-case insertion loss.

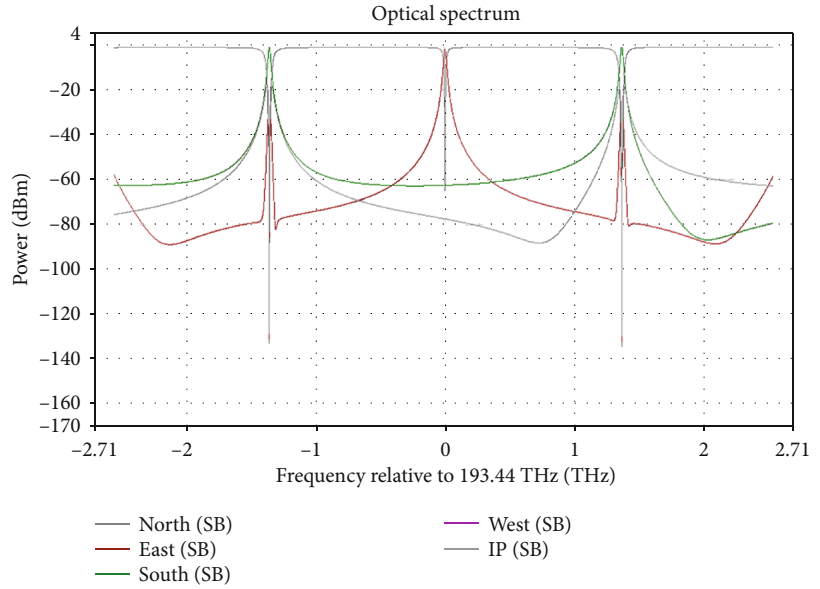

Figure 9: Power spectra of the RRW-based optical router using the default path, at all five output ports under the worst-case insertion loss.

Third, we run the simulation on the backup path of the RRW-based optical router. Similar to the simulation in the second part, the RRW-based optical router has a total of 25 MRs, 25 waveguide crossings, and 13 waveguide bends. However, in this simulation, the optical signal in the worst case will pass through four OFF-state MRs, four waveguide crossings, two bends, and two ON-state MRs. Figure 10 presents the simulation result of the worst-case insertion loss after evaluating all five communication pairs. This worst-case insertion loss happens while transmitting from West to East, too. The findings in the figure indicate that the maximum insertion loss of the RRW-based optical router when the optical signal is using the backup path is -3.6 dB for optical signal at the frequency of 193.44 THz.

Although the insertion loss increases using the backup path provided by RRW, the default path is still having an acceptable increment compared to the original router as shown in the previous figures. The figures show that the worst-case insertion loss of the default path has increased by -0.5 dB using RRW and the worst-case insertion loss using the backup path is -1.5 dB more than the default path in the original router.

Similarly, in the following two sections, we will further introduce detailed insertion loss and crosstalk noise results of more architectures in the router and the network levels.

5.4. Insertion Loss. We here evaluate more optical routers using RRW compared to others proposed in [23, 29, 30] in

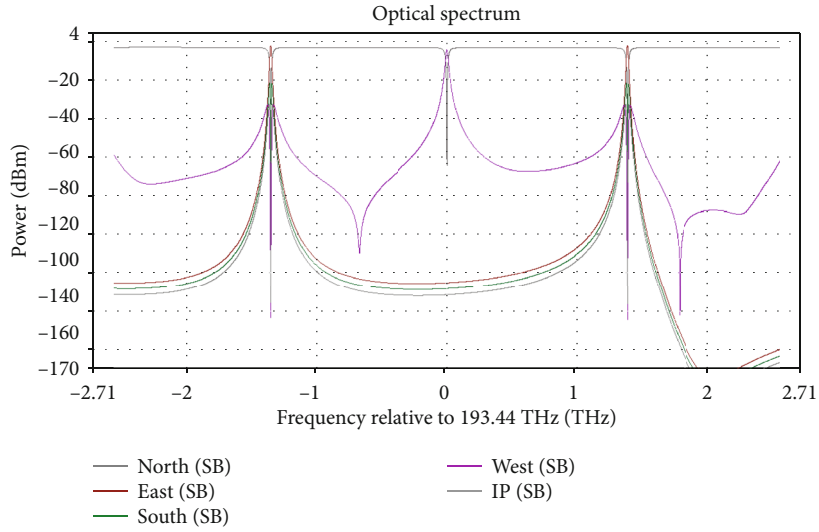

Figure 10: Power spectra of the RRW-based optical router using the backup path, at all five output ports under the worst-case insertion loss.

the same method as [40]. We evaluate the insertion loss (IL) of the other optical routers in Figure 5 and show the worst-case IL in both the default and the backup paths. Moreover, to evaluate the backup path of each router, we assume that only one MR fails at a time.

Let us, first, consider the optical routers used in 3D networks and compare them together since they have the same size. Moreover, since the NRFT and FTTDOR are based on XYZ routing algorithm, whereas the universal router in [31] and Votex in [35] are fully connected routers, we first optimize them by reducing the unused MRs of the unused communication pairs from the architecture, then implement RRW scheme. In fully connected optical routers, all input ports can communication with all output ports, whereas XYZ optical routers connect inputs with higher priority to outputs with the same priority or less priority. Thus, the routers are optimized by reducing the MRs used for unused communications, such as the communications from up to West/East/North/South.

Table 4 presents the maximum, average, and minimum port-to-port IL of all evaluated optical routers. From the table, the NRFT optical router utilizes two separated optical routers, which are a 6×6 OR and a 3×3 OR for intra- and interlayer interconnections, respectively. Therefore, the minimum port-to-port IL (-0.12 dB) would occur in the smaller router from the up port to the down port and vice versa. Similarly, the minimum port-to-port insertion loss in 7×7 FTTDOR is -0.115 dB, which occurs in the communication from the up port to the down port as well, since the up and down waveguides in FTTDOR are only connected to themselves and the IP core but not to others. Nonetheless, the minimum port-to-port insertion loss of the RRW-based optimized universal router (RO-Uni) is -0.53 dB for both the default and backup paths, and the minimum port-to-port IL of the RRW-based optimized Votex (RO-Votex) is -0.59 dB and -0.73 dB for the default path and the backup path, respectively. Although the first two mentioned routers could introduce the minimum insertion loss, routers based on our method enjoy the least average and worst-case port-to-port insertion losses. RO-Uni introduces the least average IL (-0.75 dB) in the default path and -1.101 dB IL for the backup path. On the other hand, the average ILs of RO-Votex are -0.87 dB and -1.127 dB for both the default and the backup paths, respectively. The average IL of 7×7 FTTDOR is low as well, with -0.76 dB and -0.98 dB for both the default and the backup paths, respectively. However, NRFT has the highest average IL for both the default and backup paths, with -0.93 dB and -1.48 dB, respectively. In terms of the worst-case insertion loss, RRW-based routers introduce the least IL, with -1.28 dB and -1.45 dB in RO-Votex and -0.955 dB and -1.36 dB in RO-Uni for the default and the backup paths, respectively. On the other hand, the worst-case ILs in 7×7 FTTDOR are -1.365 dB and -2.245 dB and in NRFT are -2.185 dB and -2.705 dB for the default and backup paths, respectively.

Now, we consider routers with the size of 5×5. Since the 5×5 Crux and 5×5 Cygnus are originally not fault-tolerant optical routers, thus we implement our RRW scheme and compare it with the fault-tolerant architectures designed based on them and proposed in [30]. Table 4 shows that optical routers based on RRW encounter a slightly more insertion loss in the minimum and the average insertion loss, which can be regarded as 6.6%. However, the 5×5 RRW-based optical routers encounter the least worst-case insertion loss in the back up path, with a 25% less insertion loss than the one encountered by FT-Crux and a 30.4% less insertion loss than FT-Cygnus.

Figures 11 and 12 depict the port-to-port insertion loss of FT-Crux, RRW-Crux, FT-Cygnus, and RRW-Cygnus for both the default and the backup paths. The numbers 0, 1, 2, 3, and 4 denote the ports from the injection/ejection port, North, East, South, to West, respectively. From both figures, we can notice that the maximum insertion loss of FT-Crux is mainly introduced when the signal is sent out of the injection port, whereas in FT-Cygnus, the maximum insertion loss is introduced by the North port.

Table 4: The insertion loss comparison of optical routers based on our method and other reliable optical routers for port-to-port communications.

Routers	Maximum IL (dB)		Minimum IL (dB)		Average IL (dB)	
	Default	Backup	Default	Backup	Default	Backup
7 × 7 RO-Uni	-0.955	-1.36	-0.53	-0.53	-0.75	-1.101
7 × 7 RO-Votex	-1.28	-1.45	-0.59	-0.73	-0.87	-1.127
7 × 7 FTTDOR	-1.365	-2.245	-0.115	-0.115	-0.76	-0.98
7 × 7 NRFT	-2.185	-2.705	-0.12	-0.12	-0.93	-1.48
5 × 5 RRW-crux	-0.77	-1.29	-0.23	-0.23	-0.56	-0.9
5 × 5 FT-crux	-0.71	-1.72	-0.15	-0.15	-0.51	-0.73
5 × 5 RRW-Cygnus	-0.86	-1.28	-0.28	-0.28	-0.64	-0.98
5 × 5 FT-Cygnus	-0.8	-1.84	-0.22	-0.22	-0.57	-0.94

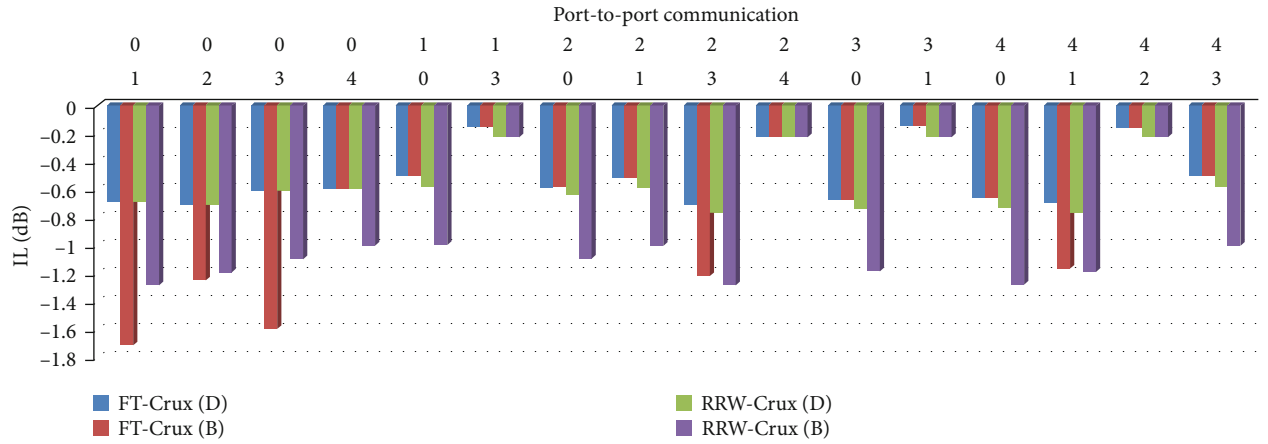

Figure 11: Port-to-port insertion loss of FT-Crux compared to RRW-Crux.

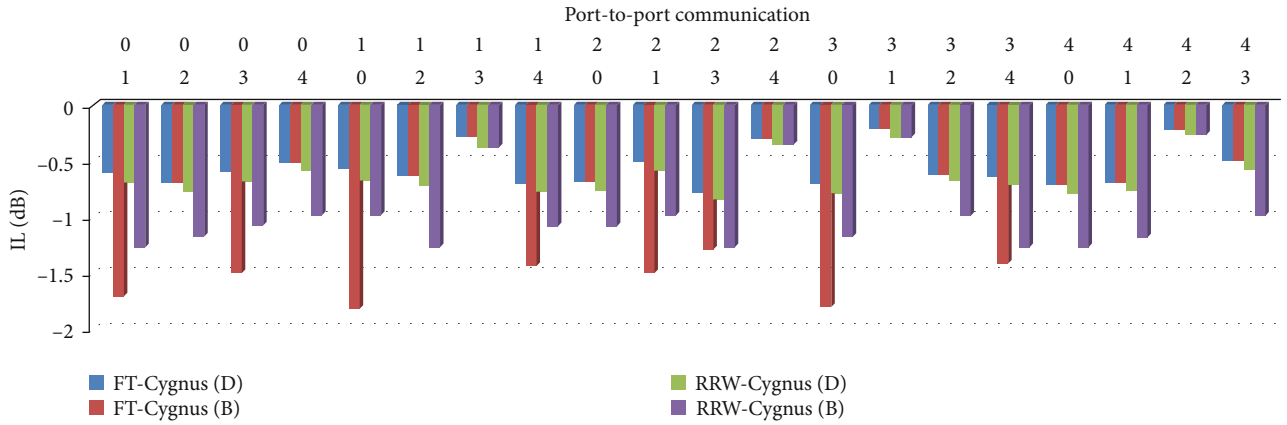

Figure 12: Port-to-port insertion loss of FT-Cygnus compared to RRW-Cygnus.

5.5. Crosstalk Noise. Here, we present the crosstalk comparisons of several optical routers; moreover, consider the worst-case OSNR of 2D mesh network using RRW and another reliable router. Similar to the previous section, the crosstalk of the longest path is obtained similar to the method in [40].

Figure 13 depicts the crosstalk noise of 7 × 7 RO-Uni default and backup paths and 7 × 7 FTTDOR default and backup paths for each port-to-port communication pair. The numbers 0, 1, 2, 3, 4, 5, and 6 are the injection/ejection port, East, down, South, West, up, and North, respectively. The results show that the RRW-based router reduces the worst-case crosstalk noise by 39.9% for the backup path and 24.55% for the default path. Furthermore, this figure reports that RO-Uni introduces the least crosstalk noise in several communication pairs.

On the other hand, Figure 14 presents the crosstalk noise of the 5 × 5 FT-Crux and 5 × 5 RRW-Crux for each communication. It is clear that the worst-case noise is introduced by

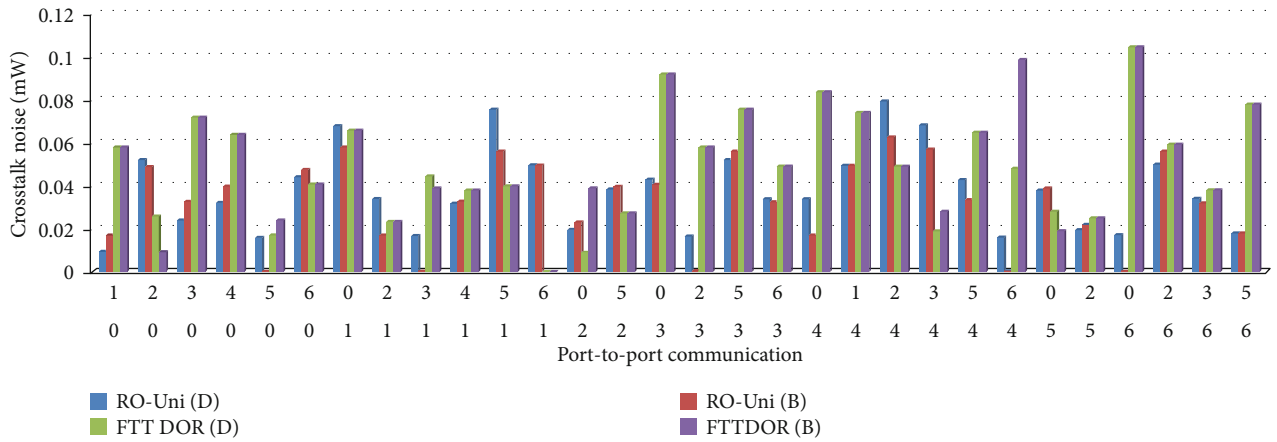

Figure 13: Port-to-port crosstalk noise of 7 × 7 optical routers compared to RRW.

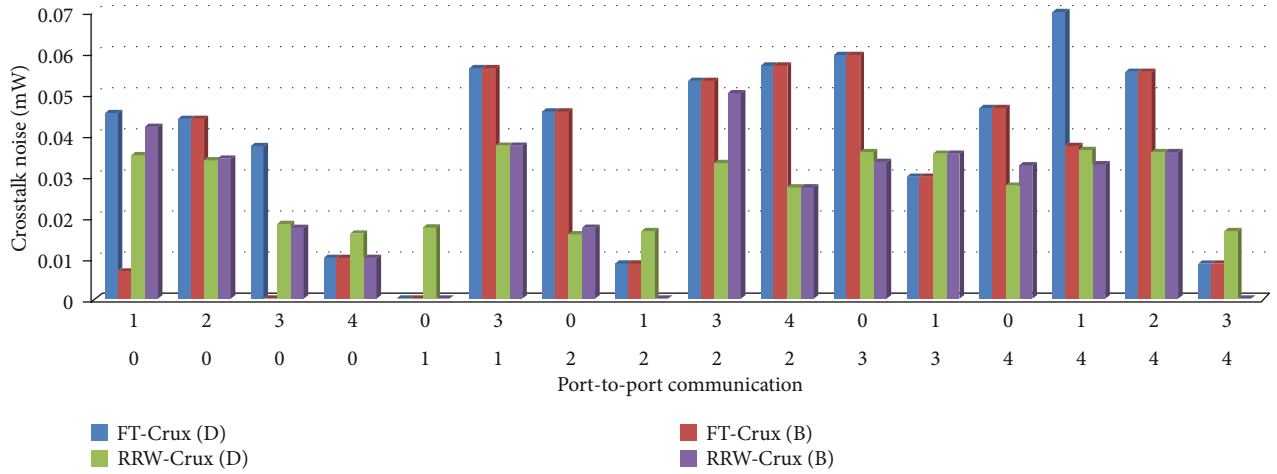

Figure 14: Port-to-port crosstalk noise of 5 × 5 FT-Crux compared to 5 × 5 RRW-Crux.

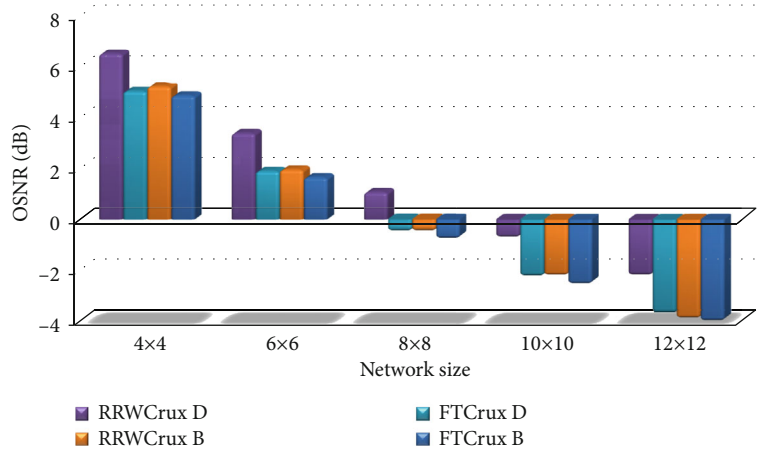

Figure 15: Worst-case OSNR of the FT-Crux and RRW-Crux optical routers for several network sizes.

FT-Crux while using the default path. The results show that the RRW-based router reduces the worst-case crosstalk noise by 46.7% for the default path and 15.7% for the backup path. Furthermore, RRW-Crux has the least crosstalk noise in many port-to-port communications.

The performance of different sizes of mesh network is evaluated using FT-Crux and RRW-Crux for several longest paths in the network and compared them to take out the worst-case crosstalk among all. Figure 15 illustrates the worst-case OSNR of FT-Crux and RRW-Crux for different

sizes of the network. The figure shows that the OSNR of FT-Crux using both the default and the backup paths and RRW-Crux using backup path is decreasing drastically as the network gets bigger in size. RRW-Crux increases the OSNR by an average of 68.5% for the default path and an average of 15.9% for the backup path compared to FT-Crux default and backup paths, respectively, for the size of 4×4, 6×6, 8×8, 10×10, and 12×12 2D mesh.

6. Conclusions

Reliability of an optical router is a hot topic for researchers. It determines the efficiency and performance of the network. We proposed a universal method that is easily implemented to an optical router for reliability purposes. The method does not expose the optical router to further contention or blocking problems. In this method, we implement a reliable ring waveguide (RRW) with a specific number of MRs, which is $2n$, to any $n \times n$ optical router to provide an alternative path for any faulty communication. Another important feature of the proposed method is that signals transmitted using the alternative path do not affect the transmitted signals using the original path. Moreover, we proposed a simultaneous transmission analysis for optical routers to show the feasibility of our method.

The results show that the failure probability of RRW-based optical routers is at most 5.19% (which is the failure probability of RRW-ODOR) compared with FTTDOR which has a failure probability of 5.79%. The simultaneous transmission in RRW-based optical routers is improved by at least 10% compared to FT-OXY and at most 46% compared to NRFT. The chapter also provides a case study by implementing RRW scheme on one of the well-known optical routers. The simultaneous results using VPIphotonics Design Suite (VPI) is providing results that are closer to fabrication. It shows that the worst-case insertion loss of the default path is increased by -0.5 dB using RRW and the worst-case insertion-loss using the backup path is increased by -1.5 dB compared to the default path in the original router. Furthermore, the worst-case insertion loss of RRW-based optical routers can be reduced by 46.34% at most for 7×7 optical routers and 30.2% at most for 5×5 optical routers. RO-Uni reduces the worst-case crosstalk noise by 24.55% and 39.9% for the default and backup paths, respectively, compared to FTTDOR. RRW-Crux reduces the worst-case crosstalk noise by 46.7% for the default path and 15.7% for the backup path compared to FT-Crux. Finally, RRW-Crux increases the OSNR by an average of 68.5% for the default path and an average of 15.9% for the backup path compared to FT-Crux default and backup paths, respectively, for the size of 4×4, 6×6, 8×8, 10×10, and 12×12 2D mesh. In the future work, we aim to combine the architecture design with a routing algorithm to further improve the network reliability.

Data Availability

All data can be obtained from the author.

Disclosure

This paper is an extended version of a previously presented one in the International Symposium on Parallel Architectures Algorithms and Programming [24].

Conflicts of Interest

The authors declare that there are no conflicts of interest regarding the publication of this paper.

Acknowledgments

This work was supported in part by the National Key R&D Program of China under Grant No. 2018YFE0202800, the National Natural Science Foundation of China under Grant Nos. 61634004 and 61934002, the Natural Science Foundation of Shaanxi Province for Distinguished Young Scholars under Grant No. 2020JC-26, and the Open Project Program of the State Key Laboratory of Mathematical Engineering and Advanced Computing under Grant No. 2019A01. This work was supported by the Youth Innovation Team of Shaanxi Universities, as well.

References

[1] M. Baharloo, R. Aligholipour, M. Abdollahi, and A. Khonsari, "*ChangeSUB*: a power efficient multiple network-on-chip architecture," *Computers & Electrical Engineering*, vol. 83, article 106578, 2020.

[2] S. Borkar, "Role of interconnects in the future of computing," *Journal of Lightwave Technology*, vol. 31, no. 24, pp. 3927–3933, 2013.

[3] Q. Cai, W. Hou, C. Yu, P. Han, L. Zhang, and L. Guo, "Design and OPNET implementation of routing algorithm in 3D optical network on chip," in *2014 IEEE/CIC International Conference on Communications in China (ICCC)*, Shanghai, China, 2015.

[4] W. Hou, G. Lei, Q. Cai, and L. Zhu, "3D Torus ONoC: topology design, router modeling and adaptive routing algorithm (invited talk)," in *2014 13th International Conference on Optical Communications and Networks (ICOCN)*, Suzhou, China, 2014.

[5] P. Guo, W. Hou, L. Guo, Q. Cai, Y. Zong, and D. Huang, "Reliable routing in 3D optical network-on-chip based on fault node reuse," in *International Workshop on Reliable Networks Design & Modeling*, Munich, Germany, 2015.

[6] S. Werner, J. Navaridas, and M. Lujan, "Designing low-power, low-latency networks-on-chip by optimally combining electrical and optical links," in *IEEE International Symposium on High Performance Computer Architecture*, Austin, TX, USA, 2017.

[7] T. Barwicz, H. Byun, F. Gan et al., "Silicon photonics for compact, energy-efficient interconnects [invited]," *Journal of Optical Networking*, vol. 6, no. 1, pp. 63–73, 2007.

[8] M. Abdollahi and S. Mohammadi, "Insertion loss-aware application mapping onto the optical Cube-Connected Cycles architecture," *Computers & Electrical Engineering*, vol. 82, article 106559, 2020.

[9] W. Yang, Y. Chen, Z. Huang, H. Zhang, H. Gu, and C. Yu, "A survey of multicast communication in optical network-on-

chip (ONoC)," in *International Symposium on Parallel Architectures, Algorithms and Programming*, Singapore, 2020.

[10] L. Guo, W. Hou, and P. Guo, "Designs of 3D mesh and torus optical network-on-chips: topology, optical router and routing module," *China Communications*, vol. 14, no. 5, pp. 17–29, 2017.

[11] S. Sun, V. Narayana, I. Sarpkaya et al., "Hybrid photonic-plasmonic non-blocking broadband 5×5 router for optical networks," *IEEE Photonics Journal*, vol. 10, no. 2, pp. 1–12, 2018.

[12] X. Shi, N. Wu, F. Ge, G. Yan, Y. Xing, and X. Ma, "Srax: a low crosstalk and insertion loss 5×5 optical router for optical network-on-chip," in *IECON - 45th Annual Conference of the IEEE Industrial Electronics Society*, pp. 3102–3105, Lisbon, Portugal, 2019.

[13] M. R. Yahya, N. Wu, Z. Fang, F. Ge, and M. H. Shah, "A low insertion loss 5 × 5 optical router for mesh photonic network-on-chip topology," in *2019 IEEE conference on sustainable utilization and development in engineering and technologies (CSUDET)*, pp. 164–169, Penang, Malaysia, 2019.

[14] M. Fadhel, H. Gu, and W. Wei, "DORR: a DOR-based non-blocking optical router for 3D photonic network-on-chips," *EICE Transactions on Information & Systems*, vol. E104.D, no. 5, pp. 688–696, 2021.

[15] R. Kappeler, *Radiation testing of micro photonic components Stagiaire Project Report*, ESA/ESTEC. Ref. No. EWP 2263, 2004.

[16] Y. Ye, Z. Wang, P. Yang et al., "System-level modeling and analysis of thermal effects in WDM-based optical networks-on-chip," *IEEE Transactions on Computer-Aided Design of Integrated Circuits and Systems*, vol. 33, no. 11, pp. 1718–1731, 2014.

[17] M. C. Meyer, A. B. Ahmed, Y. Okuyama, and A. B. Abdallah, "FTTDOR: microring fault-resilient optical router for reliable optical network-on-chip systems," in *2015 IEEE 9th International Symposium on Embedded Multicore/Many-core Systems-on-Chip (MCSoC)*, Turin, Italy, 2015.

[18] I. Datta, D. Datta, and P. P. Pande, "Design methodology for optical interconnect topologies in NoCs with BER and transmit power constraints," *Journal of Lightwave Technology*, vol. 32, no. 1, pp. 163–175, 2013.

[19] H. U. Zhan-Shuo, F. Y. Hung, K. J. Chen, S. J. Chang, W. K. Hsieh, and T. Y. Liao, "Improvement in thermal degradation of ZnO photodetector by embedding silver oxide nanoparticles," *Functional Materials Letters*, vol. 6, no. 1, p. 1350001, 2013.

[20] P. Loh and W. J. Hsu, "Design of a viable fault-tolerant routing strategy for optical-based grids," in *International Symposium on Parallel and Distributed Processing and Applications*, Berlin, Heidelberg, 2003.

[21] X. Qi, Q. Feng, Y. Chen, D. Qiang, and D. Wenhua, "A fault tolerant bufferless optical interconnection network," in *Eigth IEEE/ACIS International Conference on Computer & Information Science*, Shanghai, China, 2009.

[22] M. Tinati, S. Koohi, and S. Hessabi, "Low-overhead thermally resilient optical network-on-chip architecture," *Nano Communication Networks*, vol. 20, pp. 31–47, 2019.

[23] P. Guo, W. Hou, L. Guo et al., "Fault-tolerant routing mechanism in 3D optical network-on-chip based on node reuse," *IEEE Transactions on Parallel and Distributed Systems*, vol. 31, no. 3, pp. 547–564, 2020.

[24] M. Fadhel, L. Huang, and H. Gu, "RRW: a reliable ring waveguide-based optical router for photonic network-on-chips," in *International Symposium on Parallel Architectures, Algorithms and Programming*, Singapore, 2021.

[25] H. Li, H. Gu, Y. Yang, and Z. Zhu, "Impact of thermal effect on reliability in optical network-on-chip," *Optik - International Journal for Light and Electron Optics*, vol. 124, no. 20, pp. 4172–4176, 2013.

[26] M. Meyer, Y. Okuyama, and A. B. Abdallah, "SAFT-PHENIC: a thermal-aware microring fault-resilient photonic NoC," *The Journal of Supercomputing*, vol. 74, no. 9, pp. 4672–4695, 2018.

[27] X. Chen, M. Mohamed, Z. Li, L. Shang, and A. R. Mickelson, "Process variation in silicon photonic devices," *Applied Optics*, vol. 52, no. 31, pp. 7638–7647, 2013.

[28] Y. Xu, J. Yang, and R. Melhem, "Tolerating process variations in nanophotonic on-chip networks," in *39th Annual International Symposium on Computer Architecture (ISCA)*, Portland, OR, USA, 2012.

[29] M. Meyer, Y. Okuyama, and A. B. Abdallah, "Microring fault-resilient photonic network-on-chip for reliable high-performance many-core systems," *The Journal of Supercomputing*, vol. 73, no. 4, pp. 1567–1599, 2016.

[30] M. Abdollahi and S. Mohammadi, "Vulnerability assessment of fault-tolerant optical network-on-chips," *Journal of Parallel and Distributed Computing*, vol. 145, pp. 140–159, 2020.

[31] R. Min, R. Ji, Q. Chen, L. Zhang, and L. Yang, "A universal method for constructing N-port nonblocking optical router for photonic networks-on-chip," *Journal of Lightwave Technology*, vol. 30, no. 23, pp. 3736–3741, 2012.

[32] https://www.vpiphotonics.com.

[33] H. Gu, K. H. Mo, J. Xu, and W. Zhang, "A low-power low-cost optical router for optical networks-on-chip in multiprocessor systems-on-chip," in *2009 IEEE Computer Society Annual Symposium on VlSI*, pp. 19–24, Tampa, FL, USA, 2009.

[34] Y. Xie, M. Nikdast, J. Xu et al., "Crosstalk noise and bit error rate analysis for optical network-on-chip," in *47th ACM/EDAC/IEEE Design Automation Conference*, pp. 657–660, Anaheim, CA, USA, 2010.

[35] K. Zhu, H. Gu, Y. Yang, W. Tan, and B. Zhang, "A 3D multilayer optical network on chip based on mesh topology," *Photonic Network Communication*, vol. 32, no. 2, pp. 293–299, 2016.

[36] H. Gu, X. Jiang, and W. Zheng, "A novel optical mesh network-on-chip for gigascale systems-on-chip," in *IEEE Asia Pacific Conference on Circuits & Systems*, pp. 1728–1731, Macao, China, 2008.

[37] H. Gu, X. Jiang, and W. Zheng, "ODOR: a microresonator-based high-performance low-cost router for optical networks-on-chip," in *Proceedings of the 6th IEEE/ACM/IFIP International Conference on Hardware/software Codesign & System Synthesis*, pp. 203–208, Atlanta, GA, USA, 2008.

[38] A. W. Poon, X. Luo, F. Xu, and H. Chen, "Cascaded microresonator-based matrix switch for silicon on-chip optical interconnection," *Proceedings of the IEEE*, vol. 97, no. 7, pp. 1216–1238, 2009.

[39] J. Zhao, H. Li, H. Gu, and X. Diao, "Model-based platform for design space exploration in single-microring-based silicon photonic interconnects on chip," *Optics Communications*, vol. 453, article 124375, 2019.

[40] Y. Xie, M. Nikdast, J. Xu et al., "Formal worst-case analysis of crosstalk noise in mesh-based optical networks-on-chip," *IEEE Trans VLSI Syst*, vol. 21, no. 10, pp. 1823–1836, 2013.